Opto-Electronic Advances

CN 51–1781/TN ISSN 2096–4579 (Print) ISSN 2097–3993 (Online)

Orthogonal matrix of polarization combinations: concept and application to multichannel holographic recording

Shujun Zheng, Jiaren Tan, Hongjie Liu, Xiao Lin, Yusuke Saita, Takanori Nomura and Xiaodi Tan

Citation: Zheng SJ, Tan JR, Liu HJ, et al. Orthogonal matrix of polarization combinations: concept and application to multichannel holographic recording. *Opto-Electron Adv* **7**, 230180(2024).

https://doi.org/10.29026/oea.2024.230180

Received: 23 September 2023; Accepted: 3 November 2023; Published online: 23 October 2024

Opto-Electronic Advances

Article

October 2024, Vol. 7, No. 10

DOI: 10.29026/oea.2024.230180

Orthogonal matrix of polarization combinations: concept and application to multichannel holographic recording

Shujun Zheng[1†], Jiaren Tan[2†], Hongjie Liu[1], Xiao Lin[3], Yusuke Saita[4], Takanori Nomura[4*] and Xiaodi Tan[3*]

Orthogonal matrices have become a vital means for coding and signal processing owing to their unique distributional properties. Although orthogonal matrices based on amplitude or phase combinations have been extensively explored, the orthogonal matrix of polarization combinations (OMPC) is a novel, relatively unexplored concept. Herein, we propose a method for constructing OMPCs of any dimension encompassing 4*n* (where *n* is 1, 2, 4, 8, …) mutually orthogonal 2*n*-component polarization combinations. In the field of holography, the integration of polarization multiplexing techniques with polarization-sensitive materials is expected to emerge as a groundbreaking approach for multichannel hologram multiplexing, offering considerable enhancements in data storage capacity and security. A multidimensional OMPC enables the realization of multichannel multiplexing and dynamical modulation of information in polarization holographic recording. Despite consolidating all information into a single position within the material, we effectively avoided extraneous crosstalk during the reconstruction process. Our results show that achieving four distinct holographic images individually and simultaneously depends on the polarization combination represented by the incident wave. This discovery opens up a new avenue for achieving highly holographic information storage and dynamically displayed information, harnessing the potential of OMPC to expand the heretofore limited dimensionality of orthogonal polarization.

Keywords: orthogonal matrix of polarization combinations; polarization-modulated multiplexing; multichannel recording; polarization holography; dynamical information modulation

Zheng SJ, Tan JR, Liu HJ et al. Orthogonal matrix of polarization combinations: concept and application to multichannel holographic recording. *Opto-Electron Adv* **7**, 230180 (2024).

Introduction

Orthogonal matrices are a fundamental mathematical concept with wide-ranging applications in various scientific and engineering fields. An orthogonal matrix is a square matrix comprising rows and columns that are orthogonal unit vectors, i.e., they are normalized to a magnitude of 1 and are mutually perpendicular. Common types of orthogonal matrices include rotation matrices and Hadamard matrices. In computer graphics and com-

[1]Information Photonics Research Center, College of Photonic and Electronic Engineering, Fujian Normal University, Fuzhou 350117, China; [2]Department of Electrical and Computer Engineering, Duke University, Durham, NC 27708, USA; [3]College of Photonic and Electronic Engineering, Key Laboratory of Opto-Electronic Science and for Medicine of Ministry of Education, Fujian Provincial Key Laboratory of Photonics Technology, Fujian Provincial Engineering Technology Research Center of Photoelectric Sensing Application, Fujian Normal University, Fuzhou 350117, China; [4]Faculty of Systems Engineering, Wakayama University, 930 Sakaedani, Wakayama, 640-8510, Japan.

[†]These authors contributed equally to this work.

*Correspondence: T Nomura, E-mail: nom@wakayama-u.ac.jp; XD Tan, E-mail: xtan@fjnu.edu.cn

Received: 23 September 2023; Accepted: 3 November 2023; Published online: 23 October 2024

puter vision, orthogonal rotation matrices allow objects to be transformed while maintaining their shape and orientation[1]. In signal processing, Hadamard matrices facilitate the coding of digital signals or data sequences for error correction, separation, correlation, or encryption[2]. Moreover, numerical linear algebra heavily relies on orthogonal matrices for solving linear systems and finding least-squares solutions[3]. The importance of orthogonal matrices extends even to quantum mechanics, where they are closely linked to unitary operators representing the time evolution of quantum systems[4]. Thus, orthogonal matrices are powerful tools with exceptional properties that render them indispensable in an array of applications. The ability of these matrices to represent rigid transformations and preserve important properties during operations makes them valuable in various mathematical and computational applications.

Existing orthogonal matrices are suitable for modulating the degree of freedom with respect to amplitude or phase[5–10] but have been found to be ineffective when attempting to modulate polarization. This limitation hinders the application of orthogonal matrices for polarization modulation to some extent. Hence, a new orthogonal matrix dedicated to polarization combination is needed to expand the degree-of-freedom control of orthogonal matrices and offer a new perspective on the application of polarization modulation. This study introduces the concept of orthogonal matrices of polarization combinations (OMPC) and provides a comprehensive method for constructing nonsquare matrices belonging to multidimensional OMPC. By transitioning from the three-dimensional coordinate system to a coordinate system based on orthogonal polarization bases, a compilation of polarization combinations adhering to orthogonal relationships in distinct coordinate systems is presented. The dimensionality of polarization combinations satisfying orthogonal relationships can be considerably enhanced through the infinite expansion of polarization elements.

Multiplexing technology is a desirable method for enhancing the vast information storage capacity of holography, including angle[11–13], shift[9,14–15], orbital-angular-momentum[16–18], and polarization[19–27] multiplexing. Among the mentioned multiplexing techniques, polarization multiplexing stands out as an attractive method owing to its ability to selectively reconstruct holograms based on polarization, effectively preserving the stored information for each polarization. A recent study introduced engineering noise into the precise solution of Jones matrix elements[28], breaking through the fundamental metasurface limitation associated with polarization multiplexing, namely the dimensionality as constrained by the Jones matrix. Experiments have shown that a single metasurface can produce up to 11 independent holographic images when illuminated by visible light of different polarizations. The metasurface materials used in this method have the disadvantages of difficult processing, long time and high cost when designing special structures. Polarization-sensitive materials used in polarization holography solve these problems. Building upon the proposed OMPC in this study, we further explore its application in polarization holographic recording. The reconstruction characteristics of polarization holography play a crucial role in facilitating the implementation of polarization multiplexing[29–32]. However, the conventional polarization multiplexing method is restricted to supporting only two orthogonal states for either the signal wave or the recording reference wave. Despite the proposal of four-channel volume holographic multiplexing[20], a requirement still exists for additional orthogonal state separation of the reconstruction waves within the two orthogonal channels to facilitate the reconstruction of four holograms. Notably, the four holograms generated using this method cannot be directly differentiated solely by relying on reference waves. Consequently, the expansion of this method to encompass high-channel recording and reconstruction encounters considerable obstacles. Indeed, the proposal of OMPCs offers considerable advantages with respect to expanding the multiplexing capacity of polarization holography in the dimension of polarization. To demonstrate the advantage and effectiveness of the proposed OMPC, an experiment using $\boldsymbol{OMPC}_{2\times4}$ (an OMPC with dimensionality of four having mutually orthogonal two-component polarization combinations) is introduced in this study. The OMPC enables the recording and individual or simultaneous reconstruction of multiplex polarization holograms at a single position. Various polarization-combination vectors in the OMPC serve as the reference wave for the polarization channels during recording, allowing multiple holograms carrying different information to be recorded by the polarization interference system. Satisfying the Bragg condition, the information stored in the holograms can be reconstructed either individually or simultaneously by illuminating them with a polarization channel reference wave comprising diverse polarization-combination vec-

tors during the reconstruction process. To validate the viability of the proposed method, experiments using $\boldsymbol{OMPC}_{2\times4}$ are conducted and comprehensively analyzed. Results demonstrate the robustness and effectiveness of the method when applied to phenanthrenequinone-doped polymethyl methacrylate (PQ/PMMA) materials. The novel approach exhibits promising potential in substantially enhancing the multiplexing capacity of multi-channel holograms. This advancement of the proposed method broadens the application scope of polarization holography, particularly in the domains of optical storage and information security. OMPCs offer unprecedented opportunities for polarization holographic multi-channel multiplexing.

Construction of an orthogonal matrix of polarization combinations (OMPC)

An OMPC is a matrix describing polarized light in which each row or column vector exhibits pairwise orthogonal properties with an inner product of 0. The fundamental construction of an OMPC is illustrated in Fig. 1. The introduction commences with low-dimensional orthonormal bases. On the left side of Fig. 1, a set of orthogonally polarized lights is depicted in the x–y–z coordinate system. The x–y plane is designated as the reference incident plane; the z axis represents the propagation direction. When the oscillation direction of the polarized light remains parallel to the x–y plane, the light is called s-polarized light. Conversely, when the oscillation direction of the polarized light is perpendicular to the x–y plane, the light is called p-polarized light. The unit vectors of s-polarized and p-polarized lights can be represented using Jones vectors at polarization angles of 90° and 0°, respectively, as follows:

$$\boldsymbol{s}=\begin{bmatrix}\cos 90^\circ\\ \sin 90^\circ\end{bmatrix}=\begin{bmatrix}0\\1\end{bmatrix},\boldsymbol{p}=\begin{bmatrix}\cos 0^\circ\\ \sin 0^\circ\end{bmatrix}=\begin{bmatrix}1\\0\end{bmatrix}. \tag{1}$$

We can determine these vectors' inner products as follows: ‹$\boldsymbol{s}$, $\boldsymbol{s}$›=1, ‹$\boldsymbol{p}$, $\boldsymbol{p}$›=1, ‹$\boldsymbol{s}$, $\boldsymbol{p}$›=0. At this juncture, the s-polarized and p-polarized lights constitute a pair of orthogonally polarized lights in this coordinate system, with a dimensionality of 2.

In a coordinate system in which s- and p-polarized lights serve as the orthogonal bases, new bases are formed by these polarized lights, along with their coun-

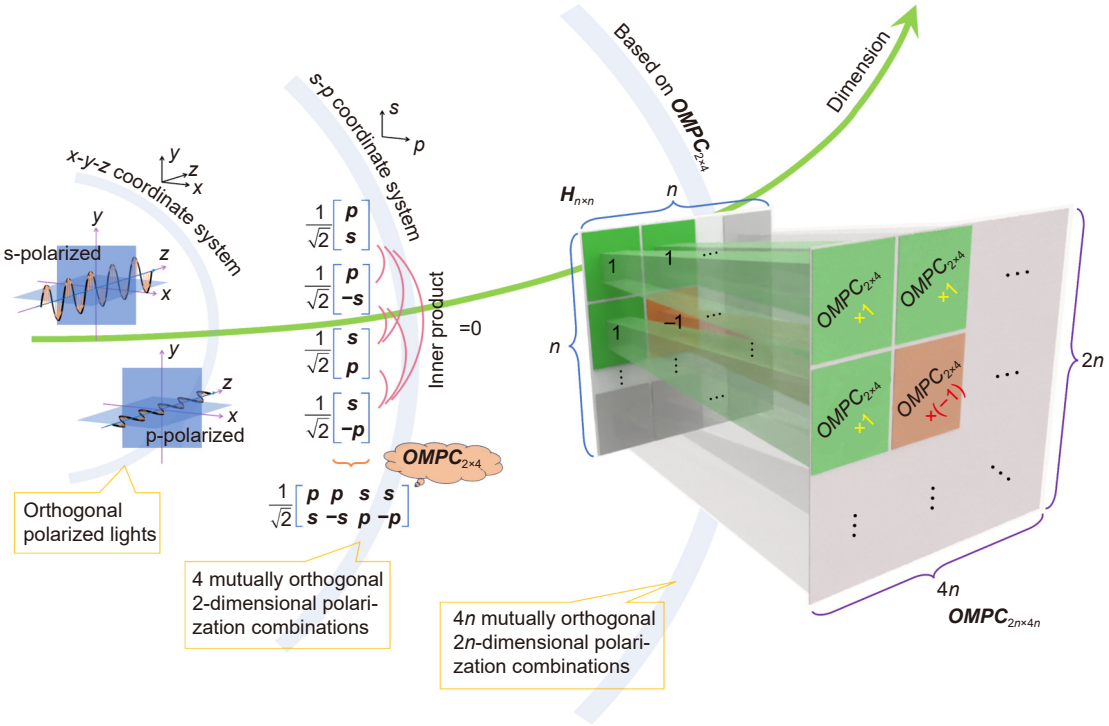

Fig. 1 | Construction schematic of arbitrary orthogonal matrix of polarization combinations (OMPC). Within the x–y–z coordinate system, only two mutually orthogonal polarized lights, namely s- and p-polarized lights, are available. Using these two orthogonal polarized lights as the bases for a new coordinate system, we can identify four mutually orthogonal 2-dimensional polarization combinations, forming the fundamental OMPC of the smallest dimensionality. Leveraging $OMPC_{2\times4}$ in conjunction with Hadamard matrices enables the generation of additional OMPCs with dimensionalities of 4n, where n is any power of 2.

terparts of opposite polarization angles, namely $\boldsymbol{s}$, $\boldsymbol{p}$, $-\boldsymbol{s}$, and $-\boldsymbol{p}$. Among these, $\boldsymbol{s}$ and $-\boldsymbol{s}$ represent linearly polarized light with polarization angles of 90° and 270°, respectively. Similarly, $\boldsymbol{p}$ and $-\boldsymbol{p}$ signify linearly polarized light with polarization angles of 0° and 180°, respectively. The unit vectors of $-\boldsymbol{s}$ and $-\boldsymbol{p}$ can be represented using Jones vectors as follows:

$$\begin{aligned} -\boldsymbol{s} &= \begin{bmatrix} \cos 270° \\ \sin 270° \end{bmatrix} = \begin{bmatrix} 0 \\ -1 \end{bmatrix}, \\ -\boldsymbol{p} &= \begin{bmatrix} \cos 180° \\ \sin 180° \end{bmatrix} = \begin{bmatrix} -1 \\ 0 \end{bmatrix}. \end{aligned} \tag{2}$$

The basic unit column vector with two elements can be derived using one pair of mutually orthogonal linearly polarized lights, such as $(\boldsymbol{p}, \boldsymbol{s})^{\mathrm{T}}/\sqrt{2}$. Subsequently, all possible two-by-two combinations from the four new bases are obtained, resulting in identifying three additional pairs of unit column vectors that constitute four pairwise orthogonal units alongside $(\boldsymbol{p}, \boldsymbol{s})^{\mathrm{T}}/\sqrt{2}$. These pairs are: $(\boldsymbol{p}, -\boldsymbol{s})^{\mathrm{T}}/\sqrt{2}$, $(\boldsymbol{s}, \boldsymbol{p})^{\mathrm{T}}/\sqrt{2}$, and $(\boldsymbol{s}, -\boldsymbol{p})^{\mathrm{T}}/\sqrt{2}$. The combination of these four column vectors results in the matrix $\boldsymbol{O}_{2\times4}$, which satisfies the condition $\boldsymbol{O}_{2\times4}{}^{\mathrm{T}}\boldsymbol{O}_{2\times4} = \boldsymbol{E}_{4\times4}$, where $\boldsymbol{E}_{4\times4}$ is the identity matrix of size 4 × 4. Hence, $\boldsymbol{O}_{2\times4}$ represents a polarization orthogonal matrix that is nonsquare and serves as the OMPC of the smallest dimensionality. We label it as $\boldsymbol{OMPC}_{2\times4}$ with a dimensionality of 4, whose expression can be written as

$$\boldsymbol{OMPC}_{2\times4} = \frac{1}{\sqrt{2}} \begin{bmatrix} \boldsymbol{p} & \boldsymbol{p} & \boldsymbol{s} & \boldsymbol{s} \\ \boldsymbol{s} & -\boldsymbol{s} & \boldsymbol{p} & -\boldsymbol{p} \end{bmatrix}. \tag{3}$$

The construction method for high-dimensional OMPC is analogous to that of Hadamard matrices[33]. By employing recursive Kronecker products, the construction of OMPCs can be extended infinitely. As depicted on the right side of Fig. 1, commencing from the foundational case of $\boldsymbol{OMPC}_{2\times4}$, the derivation of $\boldsymbol{OMPC}_{2n\times4n}$ with a dimensionality of $4n$ is achievable by leveraging the established normalized Hadamard matrix $\boldsymbol{H}_{n\times n}$ for any dimension n. The expression for $\boldsymbol{OMPC}_{2n\times4n}$ is

$$\boldsymbol{OMPC}_{2n\times4n} = \boldsymbol{OMPC}_{2\times4} \otimes \boldsymbol{H}_{n\times n}, \tag{4}$$

where "⊗" represents a recursive Kronecker product. $\boldsymbol{OMPC}_{2n\times4n}$ always satisfies $\boldsymbol{OMPC}_{2n\times4n}{}^{\mathrm{T}}\boldsymbol{OMPC}_{2n\times4n} = \boldsymbol{E}_{4n\times4n}$. The normalized Hadamard matrix $\boldsymbol{H}_{n\times n}$ can be written as

$$\begin{aligned} \boldsymbol{H}_{n\times n} &= \boldsymbol{H}_{2\times2} \otimes \boldsymbol{H}_{\frac{n}{2}\times\frac{n}{2}}, \\ \boldsymbol{H}_{2\times2} &= \frac{1}{\sqrt{2}} \begin{bmatrix} 1 & 1 \\ 1 & -1 \end{bmatrix}. \end{aligned} \tag{5}$$

As a result, $\boldsymbol{OMPC}_{2n\times4n}$ can further be described as

$$\begin{aligned} \boldsymbol{OMPC}_{2n\times4n} &= \boldsymbol{OMPC}_{2\times4} \otimes \left(\boldsymbol{H}_{2\times2} \otimes \boldsymbol{H}_{\frac{n}{2}\times\frac{n}{2}}\right), \\ \boldsymbol{OMPC}_{2\times4} &= \frac{1}{\sqrt{2}} \begin{bmatrix} \boldsymbol{p} & \boldsymbol{p} & \boldsymbol{s} & \boldsymbol{s} \\ \boldsymbol{s} & -\boldsymbol{s} & \boldsymbol{p} & -\boldsymbol{p} \end{bmatrix}, \\ \boldsymbol{H}_{2\times2} &= \frac{1}{\sqrt{2}} \begin{bmatrix} 1 & 1 \\ 1 & -1 \end{bmatrix}. \end{aligned} \tag{6}$$

When $n = 2$ in Eq. (4), where

$$\boldsymbol{H}_{1\times1} = [1], \tag{7}$$

then we can obtain

$$\begin{aligned} &\boldsymbol{OMPC}_{4\times8} = \boldsymbol{OMPC}_{2\times4} \otimes (\boldsymbol{H}_{2\times2} \otimes \boldsymbol{H}_{1\times1}) \\ &= \frac{1}{\sqrt{2}} \begin{bmatrix} \boldsymbol{p} & \boldsymbol{p} & \boldsymbol{s} & \boldsymbol{s} \\ \boldsymbol{s} & -\boldsymbol{s} & \boldsymbol{p} & -\boldsymbol{p} \end{bmatrix} \otimes \frac{1}{\sqrt{2}} \begin{bmatrix} 1 & 1 \\ 1 & -1 \end{bmatrix} \\ &= \frac{1}{2} \begin{bmatrix} \boldsymbol{p} & \boldsymbol{p} & \boldsymbol{s} & \boldsymbol{s} & \boldsymbol{p} & \boldsymbol{p} & \boldsymbol{s} & \boldsymbol{s} \\ \boldsymbol{s} & -\boldsymbol{s} & \boldsymbol{p} & -\boldsymbol{p} & \boldsymbol{s} & -\boldsymbol{s} & \boldsymbol{p} & -\boldsymbol{p} \\ \boldsymbol{p} & \boldsymbol{p} & \boldsymbol{s} & \boldsymbol{s} & -\boldsymbol{p} & -\boldsymbol{p} & -\boldsymbol{s} & -\boldsymbol{s} \\ \boldsymbol{s} & -\boldsymbol{s} & \boldsymbol{p} & -\boldsymbol{p} & -\boldsymbol{s} & \boldsymbol{s} & -\boldsymbol{p} & \boldsymbol{p} \end{bmatrix}. \end{aligned} \tag{8}$$

Clearly, the eight unit column vectors in $\boldsymbol{OMPC}_{4\times8}$ are mutually orthogonal because the inner product of each vector pair is equal to 0. Based on the $\boldsymbol{OMPC}_{2\times4}$ and the known Hadamard matrix, we can obtain an arbitrary n-valued $\boldsymbol{OMPC}_{2n\times4n}$ with $4n$-dimensional mutually orthogonal $2n$-component polarization combinations.

Multichannel polarization holographic recording using OMPC

By integrating the OMPC concept with holographic recording technology, we establish an innovative method for realizing efficient multichannel holographic image recording and reconstruction. In polarization holography, the OMPC forms the basis for both recording and decoding information. By carefully selecting suitable combinations of polarization states, we can record multiple distinct holographic images within a single medium. This advancement introduces a new avenue for multichannel information recording and retrieval.

Since its inception, polarization holography has proven effective in accurately recording and reconstructing fundamental properties, such as amplitude, phase, and polarization, using polarization-sensitive photoin-

duced anisotropic materials as the medium[29]. Herein, we exemplify the utilization of $\boldsymbol{OMPC}_{2\times4}$ for achieving four-channel multiplexing. Based on the matrix form of $\boldsymbol{OMPC}_{2\times4}$, it can be partitioned into four groups, with each group comprising two elements represented as a column vector. The design principle of multichannel polarization holograms employing these four groups of polarization-modulated waves is described in detail in Supplementary information Section 1. To fully demonstrate the characteristics of $\boldsymbol{OMPC}_{2\times4}$ akin to the inner product of an orthogonal matrix in polarization holography, it is imperative to overlap the propagation direction of each element of the reconstructed wave, thereby enabling vector superposition of the resultant reconstructed wave.

In the reconstruction stage, the respective polarization combinations of ($\boldsymbol{p}$, $\boldsymbol{s}$), ($\boldsymbol{p}$, $-\boldsymbol{s}$), ($\boldsymbol{s}$, $\boldsymbol{p}$), and ($\boldsymbol{s}$, $-\boldsymbol{p}$) are employed as the incident wave to illuminate the recorded holograms, allowing the successful reconstruction of four independent images (represented by the letters "A", "B", "C", and "D" along with adjacent circles with exceptional resolution and fidelity (Fig. 2(a–d)). Moreover, the images stored in the four holograms can be simultaneously reconstructed (Fig. 2(e) and 2(f)) under an incident wave with other polarization combinations, such as ($\boldsymbol{s}$, $\boldsymbol{s}$), ($\boldsymbol{s}$, $-\boldsymbol{s}$), ($\boldsymbol{p}$, $\boldsymbol{p}$), or ($\boldsymbol{p}$, $-\boldsymbol{p}$). The spatial positions of the reconstructed letters on each hologram remain consistent, providing evidence for the successful implementation of multichannel multiplexing at a single position.

In addition to the individual reconstruction of the four recorded holograms, a comprehensive analysis is conducted herein to examine the intensity proportions of the distinct holographic information obtained when employing incident waves with various polarization combinations for reading. The small circles in the reconstructed images on each hologram maintain a uniform size while exhibiting different spatial positions, thus enabling analysis of the reconstruction influence of the four holograms under an incident wave with different polarization combinations. To further explore the mechanism by which information is dynamically modulated, reconstruction analysis is introduced in Supplementary information Section 2. Figure 3(a) depicts the variation in the polarization state of the reference wave for reading, as its first component remains either p- or s-polarized while the polarization of its second component gradually increases from the initial polarization angle. As the polarization angle varies, the relative proportions of the four letters in holograms within the reconstructed wave also vary, as illustrated respectively in Fig. 3(b) and 3(c). The curve presented in Fig. 3(b) clearly shows that as the po-

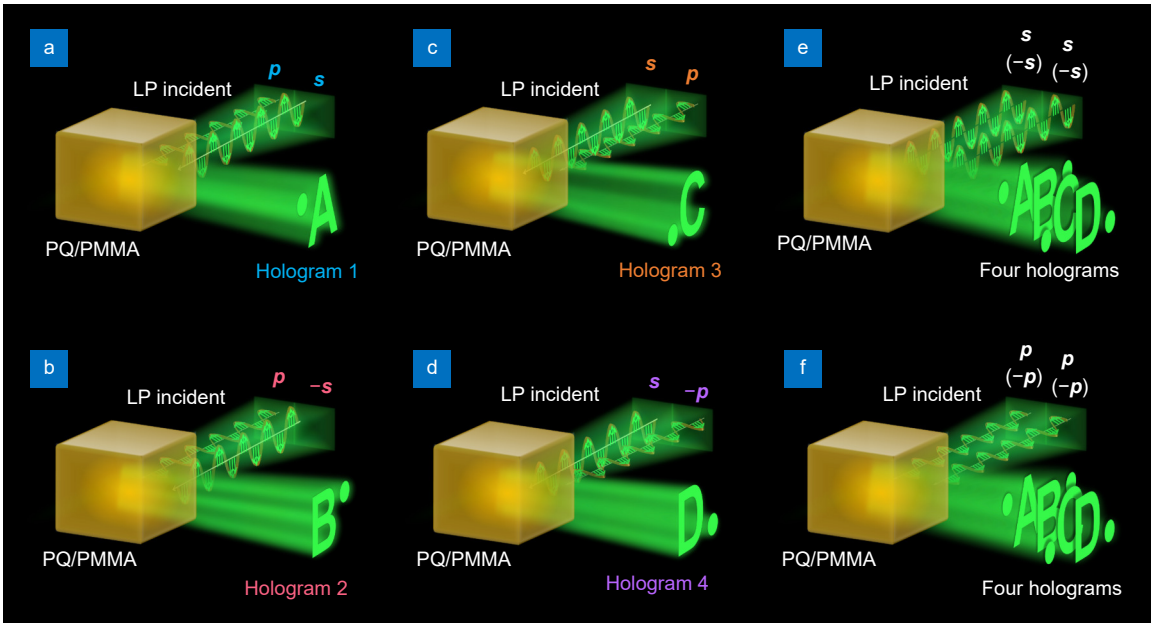

Fig. 2 | Reconstruction schematic of the designed 4-channel polarization holographic material. When the material is illuminated with incident reference waves modulated by a combination of two different polarizations, vector superposition of reconstructed wave units allows for the independent reconstruction of four holograms. (**a**–**d**) By selectively choosing the linear polarizations (LP) of incident reference waves, we can reconstruct holograms in specific polarization-combination channels while simultaneously concealing holograms in other channels. (**e**–**f**) Except for the special incident reference waves, the four stored images within the material can be simultaneously reconstructed under other incident reference waves, such as ($\boldsymbol{s}$, $\boldsymbol{s}$), ($\boldsymbol{s}$, $-\boldsymbol{s}$), ($\boldsymbol{p}$, $\boldsymbol{p}$), or ($\boldsymbol{p}$, $-\boldsymbol{p}$).

a

Increase polarization angle of the second component from different initial angle	0°	45°	90°	135°	180°	225°	270°	315°	360°
SOP of the reference wave starting at (***p***, ***s***)	(***p***, ***s***)	(***p***, ***s***−***p***)	(***p***, −***p***)	(***p***, −***p***−***s***)	(***p***, −***s***)	(***p***, −***s***+***p***)	(***p***, ***p***)	(***p***, ***p***+***s***)	(***p***, ***s***)
SOP of the reference wave starting at (***s***, ***p***)	(***s***, ***p***)	(***s***, ***p***−***s***)	(***s***, −***s***)	(***s***, −***s***−***p***)	(***s***, −***p***)	(***s***, −***p***+***s***)	(***s***, ***s***)	(***s***, ***s***+***p***)	(***s***, ***p***)

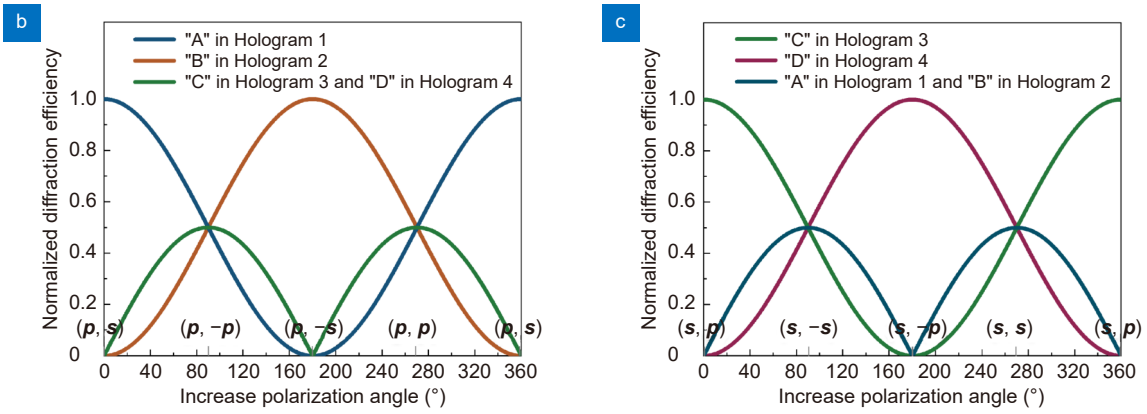

Fig. 3 | Simulated results for the four-channel polarization multiplexing holograms illuminated by reference waves with different linear polarizations for reading. (**a**) The state of polarization (SOP) of the partial reference waves for reading is depicted under either p- or s-polarization in the first component as the polarization angle in the second component gradually increases from the initial polarization angle of s- or p-polarization, respectively. (**b**) and (**c**) The reference waves employed for reading in the four-channel polarization multiplexing holograms comprise a first component that is p-polarized (or s-polarized) as well as a second component that starts from s-polarized (or p-polarized) and increases in polarization angle. The total increase in polarization angle is 360 degrees.

larization angle increases, the reconstructed image exhibits five sequential nodal points. Initially, only "A" is present, followed by a transition where "A" > "C" = "D" > "B", then "A" = "B" = "C" = "D", further transitioning to "B" > "C" = "D" > "A", and ultimately only "B" is present. When the first component of the reading reference wave is altered to be s-polarized and the polarization angle of the second component increases from its initial p-polarization, the primary images transition from "A" and "B" to "C" and "D". Figure 3(c) illustrates the trends for each reconstructed image. The sequence of image appearance evolves as follows: initially, only "C" is observed, then "C" > "A" = "B" > "D", followed by "A" = "B" = "C" = "D", subsequently transitioning to "D" > "A" = "B" > "C", and finally only "D" is present. Clearly, employing OMPC to design the multichannel polarization holograms enables dynamical reconstruction of information carried by each recorded hologram during reading with different incident waves.

Experimental demonstration

To verify the proposed method using $\boldsymbol{OMPC}_{2\times4}$, an experimental optical system was established (Fig. 4(a)). A laser beam with a wavelength λ of 532 nm (MSL-FN-532) after collimation and expansion was split into two beams using polarization beam splitter (PBS) 1 (PBS1). A rectangular aperture was used to shape the beam into a square configuration prior to its arrival at PBS1. The transmitted p-polarized beam served as the signal wave, whose amplitude information was modulated by the amplitude-modulated spatial light modulator (A-SLM) (TSLM-023-A). Subsequently, the amplitude-modulated wave traversed a 4-*f* system composed of lenses L3 and L4 before irradiating into the PQ/PMMA material[34–36]. Furthermore, another 4-*f* system comprising lenses L5 and L6 was positioned between the material and the charge-coupled device (CCD) camera (CHUM-1228C). Furthermore, the reflected s-polarized beam was used as the reference wave. In the reference wave path, the beam was once again split into two distinct polarization beams using PBS2. Half-wave plate 2 (HWP2) was used to adjust the optical intensity ratio between the two beams split by PBS2. Subsequently, these beams were combined in a nonoverlapping manner using the beam splitter (BS) after modulation using HWP3 and HWP4. The fast axes of HWP3 and HWP4 were manipulated to generate four distinct combinations of the final reference wave. Finally, the reference and signal waves underwent mutual interference at a 90° angle within the PQ/PMMA material. As depicted in Fig. 4(b), the letters "A", "B", "C", and "D" were successively recorded using polarization combinations (***p***, ***s***), (***p***, −***s***), (***s***, ***p***), and (***s***, −***p***) as the recording ref-

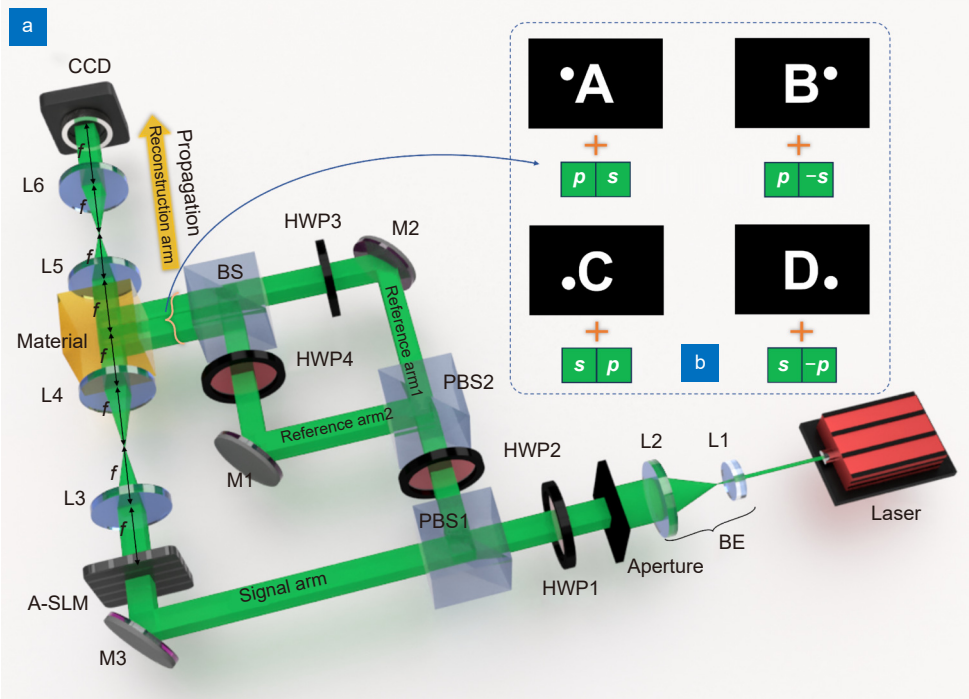

Fig. 4 | Experimental setup and specific preparation process for polarization holograms in the four-channel configurations. (**a**) Experimental setup for recording the multiplexing polarization holograms. (**b**) Recording conditions for 4-channel polarization holograms. Four exposure recordings were carried out consecutively; each exposure employed its respective polarization-combination channel to record the corresponding image. For instance, in the reference optical path, reference arms 1 and 2 were respectively modulated to be p- and s-polarized, respectively. Simultaneously, the amplitude-modulated spatial light modulator (A-SLM) on the signal optical path uploaded the image of the letter "A". Subsequently, the two beams mutually interfered in the phenanthrenequinone-doped poly (methyl methacrylate) (PQ/PMMA) material. L1–L2: lenses; BE: beam expander system composed of L1 and L2 (5× overall beam expansion); HWP1–HWP4: half-wave plates; PBS1–PBS2: polarization beam splitters; M1–M3: mirrors; BS: beam splitter; CCD: charge-coupled device.

erence waves. To modulate the reference wave into these four combinations, the fast axis directions of HWP3 and HWP4 were adjusted as follows: 0° and 0°, 0° and 90°, 45° and 45°, and 45° and 135°, respectively. The recording durations for letters "A", "B", "C", and "D" were 120, 90, 60, and 60 s, respectively.

Upon completion of the recording process, the reference waves used for reading were obtained by rotating HWP4 from its initial position of 0° or 45° while maintaining the fast axis of HWP3 at 0° or 45°, respectively, with the acquired polarization combinations as depicted in Fig. 5(a). The results of the reconstructed wave were thoroughly analyzed by examining the intensity scale of the surrounding small circles, aiding in gaining a deeper understanding of the proportions of the four holograms; these results are presented in Fig. 5(d) and 5(e). Furthermore, these results were compared with the simulation results. Additionally, Fig. 5(b) and 5(c) illustrate the reconstruction images obtained under five distinct reading reference wave illuminations, as depicted in Fig. 5(d) and 5(e), respectively. We observe that the independently recorded image could be reconstructed only when the reference wave for reading aligned with the column vector of the $\boldsymbol{OMPC}_{2\times4}$. In Fig. 5(b) and 5(c), images I, V, VI, and X correspond respectively to the results obtained when polarization combinations ($\boldsymbol{p}$, $\boldsymbol{s}$), ($\boldsymbol{p}$, $-\boldsymbol{s}$), ($\boldsymbol{s}$, $\boldsymbol{p}$), and ($\boldsymbol{s}$, $-\boldsymbol{p}$) were used for illumination. In these specific polarization combinations, the letters "A", "B", "C", and "D", respectively, were individually reconstructed. The four results of the individually reconstructed images as shown in Fig. 5(b) and 5(d) is binarized and then compared with the corresponding original images. The root-mean-square error values of "A", "B", "C", and "D" were calculated to be 0.0633, 0.0728, 0.0627, and 0.0697, respectively, after exposing the reference waves corresponding to $\boldsymbol{OMPC}_{2\times4}$. The corresponding SSIM (structural similarity index) scores were 0.9565, 0.9485, 0.9677, and 0.9539, respectively. The diffraction efficiencies of the four holograms were approximately 6×10^{-4}. However, under all other polarization combinations, all four letters occurred simultaneously, resulting in an illegible image due to information crosstalk. Similar to the simula-

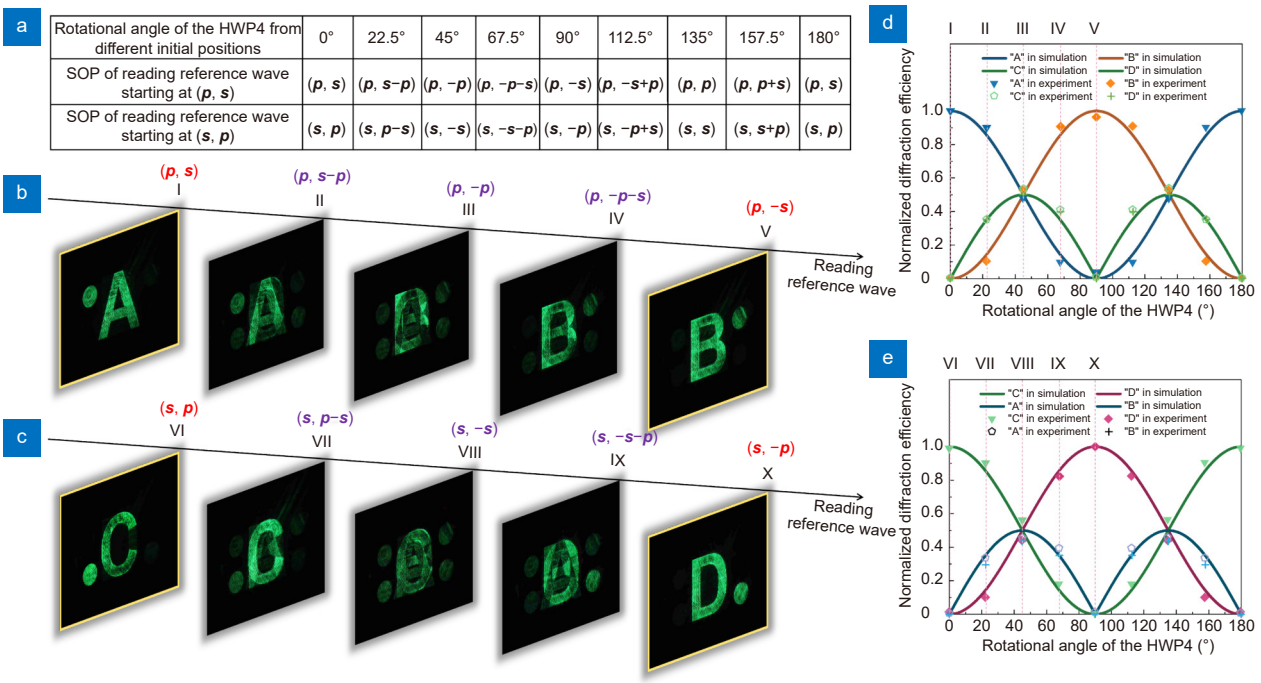

Fig. 5 | Reconstructed experimental results for the four-channel polarization multiplexing holograms, with a specific focus on the outcomes achieved when 16 different polarization combinations of reference waves were used to illuminate the holograms for reading. (**a**) State of polarization (SOP) of partial reading reference waves as a function of the rotational angle of half-wave plate 4 (HWP4) as it increased from any of its initial positions. (**b**, **e**) The reference waves employed for reading in the four-channel polarization multiplexing holograms reconstruction consisted of a first component that was (b) p-polarized or (e) s-polarized as well as a second component that transitioned from (b) s-polarized or (e) p-polarized to other linear polarizations as the rotational angle of HWP4 increased by increments of 22.5°. (**c**, **d**) Five reconstruction results showcased from the experimental datasets depicted in (b) and (e), respectively, highlighting the outcomes achieved under different reading reference waves.

tion results depicted in Fig. 2(e) and 2(f),Fig. 5(b) III and 5(e) VIII demonstrate that when exposed to their respective reference waves for reading, the letters "A", "B", "C", and "D" accounted for nearly equal proportions within the reconstructed results, as evident from the four circles surrounding the reconstructed images. The experimental results closely matched the simulation results, providing strong evidence for the accuracy and feasibility of the underlying theory in the proposed method.

We observed that the $4n$ combinations under $\boldsymbol{OMPC}_{2n\times 4n}$ could be categorized into two groups. For instance, $\boldsymbol{OMPC}_{2\times 4}$ could be categorized into one group containing ($\boldsymbol{p}$, $\boldsymbol{s}$) and ($\boldsymbol{p}$, $-\boldsymbol{s}$) and a second group containing the remaining two combinations. These two groups adhered to the traditional orthogonal state relationship. The reconstruction principle of the dual-channel recording achieved by these two groups has been previously analyzed and validated[20]. Analogous analysis of the reconstruction principles of the $2n$-channel recording achieved by the $2n$ combinations specific to the proposed method (such as ($\boldsymbol{p}$, $\boldsymbol{s}$) and ($\boldsymbol{p}$, $-\boldsymbol{s}$) for $n = 1$) is presented in Fig. S1 and S2. Further validating the feasibility of the proposed method, a 4-channel multiplexing of an OMPC ($n = 1$) was formed from the combination of the dual-channel formed by the traditional pairwise orthogonal states and the two ($n = 1$) combinations proposed in this study, which adhered to orthogonal characteristics.

Scalability to higher channel counts

A pivotal characteristic of the proposed approach is its potential to infinitely expand the modulation dimensionality of the reference wave polarization, thereby enabling the effective multiplexing of multichannel holograms. However, the size of the reference wave grows exponentially with the increasing value of n, resulting in increased complexity of the required optical setup and increased difficulty in experimental operation. In the course of scaling this technique to accommodate numerous channels, specialized devices such as spatial light modulators can be harnessed for the modulation of polarization states in the reference optical path. Moreover, to ensure and enhance the quality and efficiency of multichannel recording and reconstruction, factors that may

affect reconstruction performance must be considered. In scenarios involving consistent laser power, the intensity of the reconstructed wave hinges on the recording duration of the material, which, in turn, affects the concentration of photosensitive molecules within the medium. Prolonging the recording duration amplifies the consumption of photosensitive molecules. Conversely, lengthier recording periods aid in the distinct detection of the reconstructed wave. Achieving a harmonious balance between these two factors presents a challenge. Throughout the recording and reconstruction processes of multiple channels, compromises must be made, involving the need to relinquish one aspect to preserve the other. Throughout the experimental process, we observed that with an increase in the value of n, the diffraction efficiency progressively decreased while maintaining minimal crosstalk. However, in the domain of polarization holography, despite the reduced diffraction efficiency, successful detection by CCD remained feasible.

Conclusion

The proposed OMPC offers novel ideas, tools, and means for polarization modulation, making it possible to enhance holographic storage capacity through polarization modulation strategies. We presented the concept of OMPC and outlined an approach for its construction. We further demonstrated the application of OPMC in polarization multiplexing using polarization holography, which can achieve dynamic transformation and storage of information at a single position within a material. Our analysis results show the robustness and effectiveness of the method when applied to PQ/PMMA materials. Our approach allows for genuine polarization multiplexing, ensuring precise information reconstruction based on specific polarization combinations of the employed reference wave. During the reading process, our experimental findings unequivocally established that only the reference wave adhering to the $\boldsymbol{OMPC}_{2\times4}$ condition could attain autonomous and high-contrast reconstruction of stored information. Deviation from this criterion would result in concurrent reconstruction of multiple data items. Consequently, this approach assures the security of information storage.

This advance broadens the application scope of polarization holography, particularly in the domains of optical storage and information security. This efficient, expandable method thus offers a novel and unprecedented opportunity for achieving multiplexing of multiple polarization-selective holograms using a polarization-sensitive material. Our findings provide grounds to speculate that as the value of n increases, it becomes possible to employ $4n$ polarization-modulated reference waves for recording and reconstructing $4n$ images at one position within the material. The proposed method can also be combined with multidimensional modulation (phase and amplitude) of the signal wave[37], considerably enhancing the storage density of optical information.

References

1. Lu CP, Hager GD, Mjolsness E. Fast and globally convergent pose estimation from video images. *IEEE Trans Pattern Anal Mach Intell* **22**, 610–622 (2000).
2. Horadam KJ. *Hadamard Matrices and Their Applications* (Princeton University Press, 2012).
3. Trefethen LN, Bau III D. *Numerical Linear Algebra: Twenty-Fifth Anniversary Edition* (SIAM, Philadelphia, 2022).
4. Feynman RP, Hibbs AR, Styer DF. *Quantum Mechanics and Path Integrals* (Dover Publications, New York, 2010).
5. Wang R, Guo JB, Leung H. Orthogonal circulant structure and chaotic phase modulation based analog to information conversion. *Signal Process* **144**, 104–117 (2018).
6. Li JH, He MZ, Zheng TX, Cao LC, He QS et al. Two-dimensional shift-orthogonal random-interleaving phase-code multiplexing for holographic data storage. *Opt Commun* **284**, 5562–5567 (2011).
7. Figueroa J, Cros J, Viarouge P. Generalized transformations for polyphase phase-modulation motors. *IEEE Trans Energy Convers* **21**, 332–341 (2006).
8. Xin Y, Wang ZD, Giannakis GB. Space-time diversity systems based on linear constellation precoding. *IEEE Trans Wirel Commun* **2**, 294–309 (2003).
9. Li JH, Cao LC, Gu HR, Tan XD, He QS et al. Orthogonal-reference-pattern-modulated shift multiplexing for collinear holographic data storage. *Opt Lett* **37**, 936–938 (2012).
10. Makey G, Yavuz Ö, Kesim DK, Turnalı A, Elahi P et al. Breaking crosstalk limits to dynamic holography using orthogonality of high-dimensional random vectors. *Nat Photonics* **13**, 251–256 (2019).
11. Kinoshita N, Muroi T, Ishii N, Kamijo K, Shimidzu N. Control of angular intervals for angle-multiplexed holographic memory. *Jpn J Appl Phys* **48**, 03A029 (2009).
12. Cao LC, Wang Z, Zhang H, Jin GF, Gu C. Volume holographic printing using unconventional angular multiplexing for three-dimensional display. *Appl Opt* **55**, 6046–6051 (2016).
13. Sherif H, Naydenova I, Martin S, McGinn C, Toal V. Characterization of an acrylamide-based photopolymer for data storage utilizing holographic angular multiplexing. *J Opt A Pure Appl Opt* **7**, 255–260 (2005).
14. Yoneda N, Saita Y, Nomura T. Binary computer-generated-hologram-based holographic data storage. *Appl Opt* **58**, 3083–3090 (2019).
15. Eto T, Takabayashi M, Okamoto A, Bunsen M, Okamoto T. Numerical simulations on inter-page crosstalk characteristics in three-dimensional shift multiplexed self-referential holographic data storage. *Jpn J Appl Phys* **55**, 08RD01 (2016).

16. Jin ZW, Janoschka D, Deng JH, Ge L, Dreher P et al. Phyllotaxis-inspired nanosieves with multiplexed orbital angular momentum. *eLight* **1**, 5 (2021).
17. Ouyang X, Xu Y, Xian MC, Feng ZW, Zhu LW et al. Synthetic helical dichroism for six-dimensional optical orbital angular momentum multiplexing. *Nat Photonics* **15**, 901–907 (2021).
18. Fang XY, Ren HR, Gu M. Orbital angular momentum holography for high-security encryption. *Nat Photonics* **14**, 102–108 (2020).
19. Zang JL, Kang GG, Li P, Liu Y, Fan FL et al. Dual-channel recording based on the null reconstruction effect of orthogonal linear polarization holography. *Opt Lett* **42**, 1377–1380 (2017).
20. Zang JL, Fan F, Liu Y, Wei R, Tan XD. Four-channel volume holographic recording with linear polarization holography. *Opt Lett* **44**, 4107–4110 (2019).
21. Guo JY, Wang T, Quan BG, Zhao H, Gu CZ et al. Polarization multiplexing for double images display. *Opto-Electron Adv* **2**, 180029 (2019).
22. Koek WD, Bhattacharya N, Braat JJM, Chan VS, Westerweel J. Holographic simultaneous readout polarization multiplexing based on photoinduced anisotropy in bacteriorhodopsin. *Opt Lett* **29**, 101–103 (2004).
23. Wei HY, Cao LC, Xu ZF, He QS, Jin GF et al. Orthogonal polarization dual-channel holographic memory in cationic ring-opening photopolymer. *Opt Express* **14**, 5135–5142 (2006).
24. Barada D, Ochiai T, Fukuda T, Kawata S, Kuroda K et al. Dual-channel polarization holography: A technique for recording two complex amplitude components of a vector wave. *Opt Lett* **37**, 4528–4530 (2012).
25. Zhou SL, Liu L, Chen ZJ, Ansari MA, Chen XZ et al. Polarization-multiplexed metaholograms with erasable functionality. *J Phys D Appl Phys* **56**, 155102 (2023).
26. Ilieva D, Nedelchev L, Petrova T, Tomova N, Dragostinova V et al. Holographic multiplexing using photoinduced anisotropy and surface relief in azopolymer films. *J Opt A Pure Appl Opt* **7**, 35 (2005).
27. Li X, Chen QM, Zhang X, Zhao RZ, Xiao SM et al. Time-sequential color code division multiplexing holographic display with metasurface. *Opto-Electron Adv* **6**, 220060 (2023).
28. Xiong B, Liu Y, Xu YH, Deng L, Chen CW et al. Breaking the limitation of polarization multiplexing in optical metasurfaces with engineered noise. *Science* **379**, 294–299 (2023).
29. Nikolova L, Ramanujam PS. *Polarization Holography* (Cambridge University Press, Cambridge, 2009).
30. Kuroda K, Matsuhashi Y, Fujimura R, Shimura T. Theory of polarization holography. *Opt Rev* **18**, 374–382 (2011).
31. Wang JY, Tan XD, Qi PL, Wu CH, Huang L et al. Linear polarization holography. *Opto-Electron Sci* **1**, 210009 (2022).
32. Kuroda K, Matsuhashi Y, Shimura T. Reconstruction characteristics of polarization holograms. In *2012 11th Euro-American Workshop on Information Optics* 1–2 (IEEE, 2012);http://doi.org/10.1109/WIO.2012.6488904.
33. Yarlagadda RKR, Hershey EJ. Hadamard Matrix Analysis and Synthesis (Springer, New York, 1997).
34. Lin SH, Hsu KY, Chen WZ, Whang WT. Phenanthrenequinone-doped poly(methyl methacrylate) photopolymer bulk for volume holographic data storage. *Opt Lett* **25**, 451–453 (2000).
35. Chen YX, Hu P, Huang ZY, Wang JY, Song HY et al. Significant enhancement of the polarization holographic performance of photopolymeric materials by introducing graphene oxide. *ACS Appl Mater Interfaces* **13**, 27500–27512 (2021).
36. Lin SH, Chen PL, Chuang CI, Chao YF, Hsu KY. Volume polarization holographic recording in thick phenanthrenequinone-doped poly(methyl methacrylate) photopolymer. *Opt Lett* **36**, 3039–3041 (2011).
37. Hao JY, Lin X, Lin YK, Chen MY, Chen RX et al. Lensless complex amplitude demodulation based on deep learning in holographic data storage. *Opto-Electron Adv* **6**, 220157 (2023).

Acknowledgements

We are grateful for financial supports from National Key Research and Development Program of China (2018YFA0701800); Fujian Province Major Science and Technology Program (2020HZ01012); National Natural Science Foundation of China (NSFC) (U22A2080); and China Scholarship Council (202109107007). Shujun Zheng and Jiaren Tan contributed equally to this work.

Author contributions

All authors commented on the manuscript.

Competing interests

The authors declare no competing financial interests.

Supplementary information

Supplementary information for this paper is available at https://doi.org/10.29026/oea.2024.230180

Scan for Article PDF